Benefits of a second tandem flight phase between two successive satellite altimetry missions for assessing the instrumental stability

Michaël Ablain[1], Noémie Lalau[1], Benoit Meyssignac[2], Robin Fraudeau[1], Anne Barnoud[1], Gérald Dibarboure[3], Alejandro Egido[4], and Craig Donlon[4]

[1]MAGELLIUM, Ramonville Saint-Agne, 31520, France
[2]LEGOS, CNES, CNRS, IRD, Université Paul Sabatier, Toulouse, 31400, France
[3]CNES, Toulouse, 31400, France
[4]ESA, ESTEC, Noordwijk, 2201 AZ, The Netherlands

Correspondence: Michaël Ablain (michael.ablain@magellium.fr)

Abstract.

The five successive reference missions, TOPEX/Poseidon, Jason-1, Jason-2, Jason-3, and more recently Sentinel-6 Michael Freilich, have ensured the continuity and stability of the altimetry data record. Tandem flight phases have played a key role in verifying and ensuring the consistency of sea level measurements between successive altimetry reference missions and thus the stability of sea level measurements. During a tandem flight phase, two successive reference missions follow each other on an identical ground track at intervals of less than one minute. Observing the same ocean zone simultaneously, the differences in sea level measurements between the two altimetry missions mainly reflect their relative errors. Relative errors are due to instrumental differences related to altimeter characteristics (e.g., altimeter noise) and processing of altimeter measurements (e.g., retracking algorithm), precise orbit determination, and mean sea surface. Accurate determination of systematic instrumental differences is achievable by averaging these relative errors over periods that exceed 100 days. This enables for the precise calibration of the two altimeters. The global mean sea level offset between successive altimetry missions can be accurately estimated with an uncertainty of about $\pm$ 0.5 mm ([16-84]% confidence level). Nevertheless, it is only feasible to detect instrumental drifts in the global mean sea level exceeding 1.0 to 1.5 mm per year, due to the brief duration of the tandem phase (9 to 12 months). This study aims to propose a novel cross-validation method with a better ability to assess the instrumental stability (i.e. instrumental drifts in the global mean sea level trends). It is based on the implementation of a second tandem flight phase between two successive satellites a few years after the first one. Calculating sea level differences during the second tandem phase provides an accurate evaluation of relative errors between the two successive altimetry missions. With a second tandem phase long enough, the systematic instrumental differences in sea level will be accurately reevaluated. The idea is to calculate the trend between the systematic instrumental differences made during the two tandem phases. The uncertainty in the trend is influenced by the length of each tandem phase and the time intervals between the two tandem phases. Our findings show that assessing the instrumental stability with two tandem phases can achieve an uncertainty below ±0.1 mm yr^{-1} ([16-84]% confidence level) at the global scale, for time intervals between the two tandem phases higher than four years or more, and each tandem phase lasts at least four months. On regional scales, the gain is greater with an uncertainty of ±0.5 mm yr^{-1} ([16-84]% confidence level) for spatial scales of about 1000 km or more. With regard to the scenario foreseen for the second

phase between Jason-3 and Sentinel-6 Michael Freilich planned for early 2025, two years and nine months after the end of the first tandem phase, the instrumental stability could be assessed with an uncertainty of ± 0.14 mm yr^{-1} on the global scale, and ± 0.65 mm yr^{-1} for spatial scales of about 1000 km ([16-84]% confidence level). In order to take a larger benefit of this novel cross-validation method, this involves regularly implementing double tandem phases between two successive altimetry missions in the future.

1 Introduction

The sea level data record has been continuously calculated using multiple satellite altimetry missions since January 1993. The five successive reference missions, TOPEX/Poseidon (TP), Jason-1, Jason-2, Jason-3, and more recently Sentinel-6 Michael Freilich (S6-MF), have ensured the continuity and stability of the sea level data record. The upcoming launches of the Copernicus Sentinel-6B and Sentinel-6C satellites in the next decade are expected to maintain this continuity and stability. It is crucial to maintain the stability of the sea level data record to effectively monitor the effects of current climate change, including sea level rise and acceleration (Meyssignac et al., 2023), as well as oceanic heat uptake and the Earth energy imbalance (Hakuba et al., 2021; Marti et al., 2022, 2024).

The main sources of errors in the stability of the sea level data record have been identified and their uncertainty characterised by Ablain et al. (2019), Guérou et al. (2023) and Prandi et al. (2021). First, they are attributed to short-term time-correlated errors (< 1 year) in altimeter measurements (altimeter range, altimeter-related corrections such as sea state bias and ionosphere effects), precise orbit determination (POD), geophysical, and atmospheric corrections. Second, they arise from long-term time-correlated errors (> 5 years) in POD, in wet troposphere correction, and glacial isostatic adjustment (GIA). They are also related to uncertainties in the estimate of the sea level offset between two successive reference missions. These different sources of errors reveal an uncertainty in the trend of global mean sea level (GMSL) around $\pm$ 0.7 mm yr^{-1} ([5-95]% confidence level, CL) over a 10-year period and down to $\pm$ 0.4 mm yr^{-1} ([5-95]% CL) over a 20-year period and beyond (Guérou et al., 2023). The uncertainty in the acceleration of the GMSL is estimated to be close to 0.07 mm yr^{-2} over a 25-year period ([5-95]% CL) (Guérou et al., 2023). On a regional scale of a few hundred kilometres, uncertainties in mean sea level trends range from 0.7 to 1.3 mm yr^{-1} ([5-95]% CL) (Prandi et al., 2021). This stability performance exceeds the requirements of altimetry missions (Donlon et al., 2021).

Tandem flight phases (hereafter named "tandem phase") have played a key role in verifying and ensuring the consistency of sea level measurements between successive reference missions. The tandem phases have been implemented after the launch of each new reference mission: TP and Jason-1 (2002), Jason-1 and Jason-2 (2008), Jason-2 and Jason-3 (2016), and Jason-3 and S6-MF (2021-2022). During a tandem phase, the two successive reference missions follow each other on an identical ground track at intervals of less than one minute. Upon completion of each tandem phase, the older reference mission is moved over an alternative orbit to enhance sea level observations (Dibarboure et al., 2012).

Donlon et al. (2016, 2020) clearly explain the scientific justification and mission benefits of the tandem phase based on the recommendations of the Global Climate Observing System (GCOS). During a tandem phase, we can reasonably assume

that the ocean and atmosphere at the scales we are interested in do not vary significantly between measurements made by the two altimetry missions. Therefore, by comparing the sea level measurements from the two altimeters, the geophysical and atmospherical effects are cancelled. We can therefore accurately determine the relative errors made by both altimetry missions which are made up of several effects. The first effect arises from the instrumental differences related to the altimeter characteristics (e.g., altimeter noise, how a radar pulse interacts with the ocean surface, Dibarboure et al. (2014)) and the processing of the altimeter measurements (e.g. algorithm retracking, sea-state bias correction). The second effect stems from differences in the precise orbit determination (POD) (Couhert et al., 2015; Rudenko et al., 2023). The last effect is due to the differences in the Mean Sea Surface (MSS) in areas of strong geoid gradients (Schaeffer et al., 2023) because the two satellites are not exactly on the ground track ($\pm$ 1 km).

The systematic instrumental differences are obtained after averaging the short-term time-correlated effects on the relative errors (e.g., instrumental noise, differences in the POD and the MSS) over a period of at least 100 days (noa, 2008). Tandem phases allowed the precise calibration of the two altimeters, with the detection of systematic instrumental differences of a few millimetres to a few centimetres at different spatial scales from a few hundred kilometres to the global scale (for example, Dorandeu et al. (2004); Ablain et al. (2010); Cadier et al. (2024)). They allowed in particular the accurate estimation of the GMSL offset between two successive altimetry missions on the order of a few millimetres to a few centimetres (depending on the altimetry missions). The low level of uncertainty in the GMSL offset, close to $\pm$ 0.5 mm ([16-84]%) (Ablain et al., 2019), allows us to accurately link the GMSL time series and thus reduce the uncertainty in the GMSL trend by less than $\pm$ 0.05 mm yr^{-1} ([16-84]% CL) over a 10-year period (Zawadzki and Ablain, 2016).

However, it is only feasible to detect instrumental drifts in the global mean sea level exceeding 1.0 to 1.5 mm per year, due to the brief duration of the tandem phase (9 to 12 months). Other methods have been developed and used for more than 30 years to verify the long-term stability of altimeter measurements, within the scope of altimetry validation activities. They are based on cross-comparisons with altimetry missions together (e.g., crossover comparison, along-track comparison), on comparisons with independent measurements (e.g., ocean model reanalysis, in situ data such as tide gauge measurements), and also on the assessment of the sea level budget closure (Dieng et al., 2017; Barnoud et al., 2021). Each validation method has a specific uncertainty and the potential to detect drift in the sea level data record. For example, comparison of altimetry measurements and tide gauge data allows the detection of a trend in GMSL differences with an uncertainty of approximately $\pm$ 0.7 mm yr^{-1} ([5-95]% CL) over a 10-year period (Ablain et al., 2018; Watson et al., 2021). An instrumental drift on the TOPEX-A GMSL of about 1.5 mm yr^{-1} from 1993 to 1999 was detected with this method (Watson et al., 2015; Ablain et al., 2018). Another example is the direct comparison of the along-track sea level measurements between two altimetry missions on different orbits. It allows the detection of trends in sea level differences with an uncertainty of about $\pm$ 0.3 mm^{-1} ([5-95]% CL) on the global scale and $\pm$ 1.2 mm^{-1} ([5-95]% CL) at regional scales over a 10-year period (Jugier et al., 2022). A drift in the Sentinel-3A GMSL of approximately 1.2 mm yr^{-1} $\pm$ 0.6 m^{-1} ([5-95]% CL), from 2016 to 2021, was detected due to an error in the processing of altimeter measurements (Jugier et al., 2022). For all of these methods, the ocean is not observed at the same location and/or at the same time. As a consequence, sea level differences include part of the oceanic variability and additional errors (geophysical and atmospheric corrections, POD) not cancelled in sea level differences. Both of these effects limit our

ability to detect a drift in the altimeter measurements. The situation would be different if the satellite altimeter system and commensurate in situ fiducial measurement reference system were capable of fully sampling the same ocean variability (e.g. the same tides, waves, ocean dynamics, and their regional geographic patterns amongst other aspects).

This study aims to propose a novel cross-validation method with a better ability to assess instrumental stability. We propose the realisation of a second tandem phase between two successive altimetry missions to evaluate the relative stability of two successive altimetry missions. The fundamental concept is illustrated in Fig. 1. This entails relocating the previous altimetry mission back to its initial orbit several years after the first tandem phase. The two consecutive altimetry missions will once more be positioned less than a minute apart in identical orbit. With a second tandem phase long enough and two tandem phases separated by a time long enough, the systematic instrumental differences between the two altimetry missions will be reassessed. We can then analyse how systematic instrumental differences have changed between the first and second tandem phases by calculating the trend of sea level differences over the period that includes both tandem phases (blue line in Fig. 1).

In this paper, we demonstrate the ability of the 2-tandem phase method to assess instrumental stability. We explain the method developed to quantify the uncertainty of the 2-tandem phase method in Section 2. We assess the global uncertainty of the 2-tandem phase method, which varies depending on the length of the second tandem phase and the interval between the two phases in Section 3. Additionally, we evaluate the method's uncertainty at regional scales by examining its sensitivity to spatial scales ranging from several hundred to a thousand kilometres. Finally, we compare the uncertainty obtained with other validation methods to highlight the benefits of the second tandem phase for assessing the instrumental stability in Section 4. We also discussed the results with regard to the scenario foreseen for the second tandem phase between Jason-3 and S6-MF (Ferrier, 2023) planned for early 2025, for a duration of four months, two years and nine months after the end of the first tandem phase.

2 Methodology for estimating uncertainty in the 2-tandem phase method

This section presents the methodology developed in this study to estimate the uncertainty associated with the 2-tandem phase method. The uncertainty of the 2-tandem phase method is characterised by the uncertainty in sea level trends over the duration of both tandem phases (depicted by the blue line in Fig. 1). Our method is based on the framework established by Ablain et al. (2019) and Prandi et al. (2021), which evaluates uncertainties in trends at both global and regional scales.

2.1 Uncertainty budget assessment during a tandem phase

Initially, the methodology involves establishing an uncertainty budget for sea level differences within a tandem phase. The uncertainty budget for the Global Mean Sea Level (GMSL), as described in Ablain et al. (2019), pinpoints various error sources in altimetry data, such as environmental corrections, precise orbit determination (POD), instrumental noise, instrumental drift and offset, which contribute to the uncertainties of the GMSL series. The uncertainty budget also provides the statistical properties of these errors, including the temporal correlation and standard deviation for each error source. During a tandem phase, the uncertainty budget for sea level differences is significantly simplified since most uncertainties included in the mean

125 sea level uncertainty budget are canceled out (e.g., geophysical and atmospheric corrections, long-term time-correlated effects in POD). It only covers uncertainties arising from short-term time-correlated effects previously stated in the Introduction, which result from sea level differences in altimeter measurements, the POD, and the mean sea surface between two altimeter missions.

2.1.1 Mean sea level differences calculation during the tandem phase

130 We calculate the sea level estimates over the three tandem phases between Jason-1 and Jason-2 (August 2008 - January 2009), between Jason-2 and Jason-3 (February 2016 - October 2016) and between Jason-3 and S6-MF (September 2021 - April 2022). It should be mentioned that the tandem phase between Jason-3 and S6-MF started on 17 December 2020 and ended on 4 April 2022. However, an instrumental anomaly was detected on side A of the S6-MF altimeter (Poseidon-4) a few months after the launch of S6-MF. Thus, on 14 September 2021 a switch was operated on side B of the S6-MF altimeter (Dinardo et al.,

135 2022). Therefore, the data of the first tandem phase between S6-MF and Jason-3 can be used after the side B change from 14 September 2021 to 4 April 2022. For Jason-1, Jason-2, and Jason-3, the altimeter products used are the non-time critical (NTC) along-track level-2+ (L2P) products from the Copernicus Marine Service under the CNES responsibility. These products are downloaded from the Aviso ftp website (http://ftp-access.aviso.altimetry.fr/uncross-calibrated/open-ocean/non-time-critical/l2p/sla/) and contain the along-track sea level anomaly at 1Hz (SLA, see Eq. 1) calculated after applying a validation

140 process fully described in the product handbook of each altimetry mission (Along-track Level-2+ (L2P) Sea Level Anomaly Sentinel-3 / Jason-CS-Sentinel-6 Product Handbook, 2022). We use version 03_00 which is the current product version of Sentinel-3 and S6-MF L2P, with respective reprocessing from Baseline Collection 004 (PB2.61) and Baseline Collection F05. The along-track SLA provided in the L2P products is derived from the following equation:

$$SLA = Orbit - Range - \Sigma_i Correction_i - Mean\,Sea\,Surface \tag{1}$$

145 where $Orbit$ is the radial distance between the satellites and the geoid, $Range$ the distance between the satellite and the sea surface, $\Sigma_i Correction_i$ are the sum of the geophysical and atmospheric corrections to be applied (e.g. ocean, polar and earth tides, wet and dry troposphere corrections, sea state bias correction,...), $Mean\,Sea\,Surface$ is the mean of the sea surface height from which sea level anomalies are derived. The geophysical corrections applied in L2P products for the SLA calculation are already homogenised for each altimetry mission and identical during a tandem phase. We have also verified that

150 whether or not geophysical and atmospheric corrections are applied, the sea level estimates remain consistent during a tandem phase. It should also be noted that the wet troposphere correction derived from microwave radiometers has not been applied to the sea level calculation to avoid the introduction of instrumental errors not related to the altimeter measurements.

  We have calculated the GMSL differences between two altimeter missions during a tandem phase applying the GMSL AVISO method described in Henry et al. (2014). In summary, the 1 Hz SLA measurements along track have been first averaged

155 within grid cells for each orbital cycle ($\approx$ 9.91 days for reference altimetry missions). We have made this computation for each altimeter mission separately. As recommended by Henry et al. (2014), cells of 1° latitude per 3° longitude have been applied to optimise the effect of sea level variability observed by reference altimetry missions in the GMSL. Then we have calculated

the SLA differences at regional scales for each cycle of the tandem phase, calculating directly the differences between the SLA grids of each altimeter mission. The time serie of GMSL differences has then been obtained after spatially averaged the grids of SLA differences at each cycle, with a weighting that accounts for the relative ocean area covered.

2.1.2 Uncertainty budget on the global scale

To characterise uncertainties arising from short-term time-correlated effects, we analysed GMSL differences during tandem phases of Jason-1/Jason-2, Jason-2/Jason-3, and Jason-3/Sentinel-6 Michael Freilich (S6-MF) (over the side B period). This involved calculating the standard deviation and time correlation of the GMSL differences. We plotted these differences in the middle panel of Fig. 2. During the Jason-3/S6-MF tandem phase, the GMSL differences exhibit a 2-month periodic signal. Cadier et al. (2024) recently identified that this signal arises from beta-prime dependencies in the Centre National d'Études Spatiales (CNES) POD solution used for S6-MF. Furthermore, Cadier et al. (2024) demonstrated that using Jet Propulsion Laboratory (JPL) POD solutions substantially reduces this signal. Assuming that the identified beta-prime dependencies will be fully corrected in the updated S6-MF CNES POD, we removed this 2-month periodic signal before calculating the standard deviation of the GMSL differences. This reduced the standard deviation from 0.99 mm to 0.48 mm, providing a more realistic value. The GMSL differences before removing this periodic signal is shown by the dashed line in the middle right panel of Fig. 2. The standard deviations derived from the three tandem phases are within 0.07 mm for Jason-2/Jason-3 (0.41 mm) and Jason-3/S6-MF (0.48 mm). However, the standard deviation is slightly higher for Jason-1/Jason-2 (0.69 mm), most likely due to additional errors in the precise orbit calculation of Jason-1.

The autocorrelation of each GMSL difference, shown in the bottom panel of Fig. 2, does not exhibit a significant autocorrelation at any lag. The number of independent measurements (n) of GMSL differences, displayed in the legend of Fig. 2 (bottom panel), was calculated following the methodology of Guérou et al. (2023). This method uses the following equation:

$$n = \frac{(1 - \rho_1)}{(1 + \rho_1)} \cdot n_{\text{sample}} \tag{2}$$

where ρ_1 is the first-lag autocorrelation coefficient, representing the correlation between consecutive measurements, and n_{sample} is the total number of measurements of the sample. For all three tandem phases, the number of independent measurements is high. For S6-MF and Jason-3, $n = 18$ for a total of $n_{sample} = 20$, implying that GMSL differences largely decorrelate after approximately 3 measurements, or 30 days (one measurement per cycle). On the basis of these analyses, we assume that the GMSL differences are fully decorrelated beyond one month during these three analysed tandem phases. Therefore, the uncertainty budget of the GMSL differences during a tandem phase was established by incorporating a single 1-month time-correlated error with a standard deviation of 0.5 mm (see Tab.1). Each tandem phase yields similar but not identical results. This can be attributed to differences in the GMSL between the altimetry missions and the relatively short duration (approximately 6 to 9 months) of the tandem phases. To assess the sensitivity of our results to these factors, a sensitivity analysis was conducted (see section 3) by varying the temporal correlation from 0 to 2 months and the standard deviation of the GMSL differences from 0.4 to 0.6 mm.

2.1.3 Uncertainty budget at regional scales

The uncertainty budget for sea level differences, established on a global scale in Section 2.1.2, can be adapted to regional scales ranging from a few hundred to a few thousand kilometres. This regional adaptation is based on the framework presented by Prandi et al. (2021) for regional sea level uncertainty. As on the global scale, most of the different sources of uncertainties outlined in Prandi et al. (2021) cancel out when considering sea level differences during a satellite altimeter tandem phase. Therefore, the uncertainty budget of regional sea level differences during a tandem phase contains only uncertainties due to short-term time-correlated errors. To quantify this uncertainty, regional sea level differences between Jason-3 and S6-MF were computed during their tandem phase. Differences were calculated for varying cell sizes, from 3 ° x 3 ° to 36 ° x 36 ° (corresponding to approximately 300 km x 300 km to 4000 km x 4000 km). The standard deviation of these differences was then calculated within each cell size. This standard deviation, representing the uncertainty due to 1-month correlated errors, was incorporated into the regional uncertainty budget (see Table 2), homogeneously to the uncertainty budget at global scale.

2.2 Error covariance matrix

After specifying the uncertainty budget, the error covariance matrix for sea level differences observed during a tandem phase (Σ_{tp}, where tp stands for tandem phase) is derived using the methodology outlined in Ablain et al. (2019). The uncertainty budget contains only one source of uncertainty with short-term time-correlated errors. The covariance matrix has been modelled applying a Gaussian attenuation function determined by the wavelength of the time-correlated errors, expressed as $e^{-\frac{1}{2}\left(\frac{t}{\lambda}\right)^2}$, where the correlation timescale λ is set to 1 month (see Section 2.1.2). The resulting covariance matrix has a diagonal structure with smaller off-diagonal terms.

The error covariance matrix of the relative errors observed during the two tandem phases, Σ, is partitioned into two distinct diagonal blocks: the error covariance matrix for the first tandem phase (Σ_{tp_1}) and the second tandem phase (Σ_{tp_2}), as shown below.

$$\Sigma = \begin{pmatrix} & & & 0 & \ldots & 0 \\ & \Sigma_{tp\_1} & & \vdots & \ddots & \vdots \\ & & & 0 & \ldots & 0 \\ \hline 0 & \ldots & 0 & & & \\ \vdots & \ddots & \vdots & & \Sigma_{tp\_2} & \\ 0 & \ldots & 0 & & & \end{pmatrix} \tag{3}$$

Since the second tandem phase has not yet been executed, we assume the same error characteristics (standard deviation and temporal correlation) as those of the first tandem phase. Both tandem phases involve the same altimeter systems (e.g., Jason-3 and S6-MF), and factors such as instrumental noise, POD and mean sea surface are expected to remain consistent across both phases. Therefore, the error characteristics can reasonably be assumed to be similar.

2.3 Mathematical formalism to derive uncertainty in trends

Finally, we use this error covariance matrix (Σ) to calculate the uncertainty of the trend in sea level differences. The formalism used is also based on Ablain et al. (2019). The trend is fitted from a linear regression model ($\boldsymbol{y} = \boldsymbol{X}\beta + \epsilon$) applying an ordinary least squares (OLS) approach where the estimator of β with the OLS, noted $\hat{\beta}$, is:

$$\hat{\beta} \sim (\boldsymbol{X}^t \boldsymbol{X})^{-1} \boldsymbol{X}^t \boldsymbol{y} \tag{4}$$

Where $\boldsymbol{X}$ is the time vector that contains the date of each altimeter cycle during the two tandem phases, $\boldsymbol{y}$ is the observation vector that contains the sea level differences averaged over each complete cycle. The uncertainty of the trend is given by $\hat{\beta}$, which is the distribution of the estimator following a normal law:

$$\hat{\beta} = N(\beta, (\boldsymbol{X}^t \boldsymbol{X})^{-1}(\boldsymbol{X}^t \Sigma \boldsymbol{X})(\boldsymbol{X}^t \boldsymbol{X})^{-1}) \tag{5}$$

It should be noted that the calculation of trend uncertainty does not depend on sea level differences ($\boldsymbol{y}$), but only depends on the time vector ($\boldsymbol{X}$) and the error covariance matrix (Σ). This allows us to analyse the uncertainty of the 2-tandem phase method even though the second tandem phase has not yet been performed. This study is based on the assumption that the uncertainty budget of the second tandem phase will be the same as that of the first.

3 Uncertainty of the 2-tandem phase method

3.1 On the global scale

The uncertainty of the trend in sea level differences of the 2-tandem phase method is calculated on the global scale with the uncertainty budget described in Tab. 1. The uncertainty budget in this study is constructed by taking the U_σ for Jason-3/S6-MF. The duration of the first tandem phase is set at 6 months, corresponding to the duration of the tandem phase between Jason-3 and the altimeter side-B of S6-MF (September 14, 2021 to April 07, 2022). For the second tandem phase, we analyse the impact on the trend uncertainty of both the duration of the second tandem phase and the time elapsed since the first tandem phase. To construct the error covariance matrix (Σ, see Eq. 3), we use the same uncertainty budget for both tandem phases (see Tab. 1). Fig. 3 shows the evolution of the uncertainty of the trend in GMSL differences as a function of the time period between the two tandem phases (between 1 and 6 years), for four different time spans of the second tandem phase (from 1 month to 6 months). For a 1-year time span between the two tandem phases, the uncertainties range from 0.27 mm yr^{-1} for a second phase duration of 6 months to 0.41 mm yr^{-1} for a second phase duration of 1 month. They are reduced to about 0.12-0.16 mm yr^{-1} after 3 years between the two tandem phases. They are less than 0.10 mm yr^{-1} after 5 years between the two tandem phases with a interval of 0.02 mm yr^{-1}. These results show that the uncertainty of the trend in the GMSL differences is less influenced by the duration of the second tandem phase when the time elapsed between the two tandem phases increases. For

instance, for a time span of two years, the uncertainties in the trend are ranging from 0.24 to 0.16 mm yr^{-1} for a second tandem phase respectively from 1 month to 6 months. Whereas for a time span of five years, the uncertainties in the trend are ranging from 0.10 to 0.08 mm yr^{-1}. On the basis of these results, it is recommended that the second tandem phase be carried out as far as possible from the first (at least a few years later), but it is not necessary for this second phase to be very long. A period of 4 months is considered sufficient to verify the instrumental stability on the global scale.

It should be noted that similar analyses carried out before the launch of S6-MF led to the same recommendation (Ablain et al., 2020). It helped space agencies specify a scenario for the second tandem phase between Jason-3 and S6-MF. The second tandem phase should start in January 2025 for a duration of 4 months, 2 years, and 9 months after the first tandem phase (Ferrier, 2023). This adopted scenario is shown with a star in Fig. 3. It leads to an uncertainty of the trend in GMSL differences of 0.14 mm yr^{-1}.

The results we obtained are contingent upon how the uncertainty budget of sea level differences is specified during a tandem phase (see Tab. 1). As previously stated, the uncertainty budget may be subject to minor modifications depending on the length of the tandem phase and the altimeter missions involved. Thus, we performed a sensitivity analysis by varying the temporal correlation from 0 to 2 months and varying the standard deviation of SSHA differences between 0.4 and 0.6 mm within the uncertainty budget. The uncertainties in the trend range from 0.06 to 0.18 mm yr^{-1} when only the temporal correlation is altered, and from 0.11 to 0.17 mm yr^{-1} when only the variance is varied, in the case of the scenario adopted between S6-MF and Jason-3 for the second tandem phase. In the worst case, corresponding to a temporal correlation of 2 months and a variance of 0.6 mm, the maximum uncertainty on the trend is 0.21 mm yr^{-1}. This sensitivity analysis in the uncertainty budget indicates a low sensitivity in the absolute value of the trend uncertainty ($\pm$ 0.07 mm yr^{-1}).

3.2 At regional scales

The uncertainty of the trend in sea level differences of the 2-tandem phase method is calculated at regional scales with the uncertainty budget described in Tab. 2. The duration of the first tandem phase remains fixed to six months. We also fixed the duration of the second tandem phase to four months. We also use the same uncertainty budget for both tandem phases specified at regional scales (see Tab. 2) to construct the error covariance matrix (Σ, see Eq. 3). Different spatial scales are analysed with cell sizes ranging from 3° x 3° (330 km x 330 km) to 36° x 36° (4000 km x 4000 km). Fig. 4 shows the evolution of the uncertainties of the trend in regional mean sea level differences for these different configurations as a function of the time elapsed between the two tandem phases. Uncertainties decrease with increasing cell size. After 2 years and 9 months, corresponding to the scenario adopted for the second tandem phase between S6-MF and Jason-3, the uncertainty ranges from 1.1 mm for a size box of 3° x 3° (330 km x 330 km) to 0.4 mm for a size box 36° x 36° (4000 km x 4000 km). Detecting trends in regional mean sea level differences less than 1 mm yr^{-1} is possible in almost all ocean basins with a second tandem phase as early as two years after the first.

4 Comparison with other validation methods

4.1 Uncertainty budgets of other validation methods

To assess the uncertainty of the 2-tandem phase method, we compare it with two established approaches: a) sea level comparisons between two altimetry missions on different orbits (hereafter, the without-tandem phase method) (Jugier et al., 2022), and b) sea level comparisons between altimeter and tide gauge data (Valladeau et al., 2012; Watson et al., 2015). These methods were selected because their ability to detect drift in GMSL has previously been demonstrated using uncertainty budgets similar to the approach employed in this study (see Section 2). For the without-tandem phase method, the uncertainty budget developed by Jugier et al. (2022) was used. This budget, presented in Table A1 for the global scale and Table B1 for regional scales, accounts for the spatial and temporal differences (e.g. typically a few days and a few dozen kilometres) inherent in altimetry measurements from altimeter missions over different orbits. These differences introduce uncertainties related to geophysical and atmospheric effects, oceanic variability, and long-period time-correlated errors in the POD. Similarly, the uncertainty budget for altimeter-tide gauge comparisons, presented in Ablain et al. (2018), accounts for spatial and temporal differences between tide gauges and altimetry measurements (e.g. typically a few hours and a few dozen kilometres). Furthermore, all the errors performed by two independent system measurements are not cancelled in the sea level differences. The uncertainty budget, presented in Table C1 for the global scale, includes uncertainties associated with geophysical and atmospheric effects, oceanic variability, and long-period time-correlated errors in both altimetry (e.g., POD) and tide gauge records (e.g., land motion correction). This limitation arises primarily from uncertainties in tide gauge records, including vertical land motion due to tectonic activity and subsidence, and the spatial offset between tide gauges and altimetry measurements (Valladeau et al., 2012; Watson et al., 2021). However, highly accurate local comparisons are possible in regions with well-referenced tide gauges, such as those described by Mertikas et al. (2021).

4.2 On the global scale

In Fig. 5, the uncertainties have been plotted for the three validation methods (2-tandem phase, without-tandem phase, altimeter-tide gauges) as a function of the time spent between the two tandem phases of Jason-3 and S6-MF. The duration of the second tandem phase has been set at four months, according to the adopted scenario Ferrier (2023). It is also worth noting that the total duration of the time series used to calculate the uncertainties for all methods includes the duration of both tandem phases. This means that for 1 year spent between the two tandem phases, the total length of the time series is 1 year and 10 months (1 year + 6 months + 4 months). Similarly, for the adopted scenario of a second tandem phase of 4 months, 2 years, and 9 months after the first of 6 months, the total duration of the analysed time series is 3 years and 7 months. The analysis in Fig. 5 clearly shows that the 2-tandem phase method significantly reduces the uncertainties of the trend in the GMSL differences. Over a period of 3 years and 7 months, which corresponds to the adopted scenario, the uncertainty is 1.2 mm yr^{-1} with the tide gauge method. It is reduced to 0.42 mm yr^{-1} for the without tandem phase method, whereas with the new 2-tandem phase method, the uncertainty decreases to 0.14 mm yr^{-1}. Increasing the time spent between the two Jason-3/S6-MF tandem phases to 4 years, and hence the total duration to 4 years and 10 months, leads to lower uncertainties for each method at 0.9 mm yr^{-1},

0.35 mm yr^{-1} and 0.1 mm yr^{-1} respectively. These results highlight the better ability of the two-tandem-phase method to assess instrumental stability on the global scale.

4.3 At regional scales

Similarly to the global scale, we compare the 2-tandem phase method with the method based on sea level comparisons between two altimetry missions on different orbits (outside a tandem phase). In Fig. 6 we evaluate the evolution of the uncertainty of the trend in the regional mean sea level differences of the two methods with the time elapsed between two tandem phases, after selecting size boxes of 9° x 9° (about 1000 km). As uncertainties are not spatially homogeneous (see Fig. A1), we have also plotted in Fig. 6 the envelope of the spatial distribution of uncertainties at values between the 16th and 84th percentile (i.e., 1-σ). For a cell size of 9° by 9° (about 1000 km by 1000 km), the uncertainty at 1-σ ranges from 1.8 to 4.8 mm, with a median of 2.3 mm. We observe that the average value of trend uncertainty is even more significantly reduced at regional scales than on the global scale with the 2-tandem phase method. By conducting the analysis over 3 years and 7 months, corresponding to the adopted scenario of a second tandem phase 2 years and 9 months after the initial one, the trend uncertainty of sea level differences is 4.0 mm yr^{-1} without tandem phase, while with the new 2-tandem phase method the uncertainty decreases to 0.65 mm yr^{-1}. Increasing the total duration of the analysis to 4 years and 10 months (corresponding to 4 years between the two tandem phases of Jason-3 and S6-MF) results in lower uncertainties for each validation method, 3.0 and 0.5 mm yr^{-1}, respectively. Significantly better results obtained at regional scales are mainly explained by the effect of ocean variability. As mentioned above, it is a significant source of uncertainty when measurements are not collocated in time and space. At regional scales, the effect of ocean variability is not spatially averaged and becomes a major source of uncertainty. As the 2-tandem phase method is not affected by this effect, its ability to assess instrumental stability on regional scales is very promising.

5 Conclusions

We have proposed a novel cross-validation method to assess the instrumental stability, based on the realisation of a second tandem phase between two successive reference missions a few years after the initial one. We have demonstrated the ability of the 2-tandem phase method to assess the instrumental stability. Assuming a second tandem phase with a minimal duration of four months, it will be possible to assess on the global scale the instrumental stability with an uncertainty of less than $\pm$ 0.1 mm yr^{-1} in a CL of [16-84]% for time periods between the two tandem phases of four years and beyond. This means tree to eight times better than with the other validation methods based, respectively, on sea level comparisons outside a tandem phase and on altimetry and tide gauge comparisons. On regional scales, the gain is greater with an uncertainty of $\pm$ 0.5 mm yr^{-1} in a CL of [16-84]% for spatial scales of about 1000 km, that is six times better than with the method based on sea level comparisons outside a tandem phase. The 2-tandem phase method could be applied for the first time between S6-MF and Jason-3 after the realisation of the second tandem phase early in 2025. On the global scale and for the scenario adopted for the second tandem phase between Jason-3 and S6-MF, it will be possible to assess sea level stability with an uncertainty of $\pm$ 0.14 mm yr^{-1} in a CL of [16-84]%. On regional scales, it will be possible to assess sea level stability with an uncertainty of $\pm$ 0.65 mm yr^{-1} in

a CL of [16-84]% for spatial scales of about 1000 km. To date, we have assumed that the uncertainty budget of relative errors will be the same over the two tandem phases between S6-MF and Jason-3. It should be re-evaluated after the completion of the second tandem phase, and the uncertainties in the trend may be updated. If a significant instrumental drift in sea level is detected, it cannot automatically be attributed to the S6-MF or Jason-3 altimetry missions. In-depth investigations will have to be carried out by experts from the two satellites, and alternative validation methods will also have to be implemented, even if they are less accurate at detecting a drift in altimeter measurements. These inquiries could lead to revisions in the mean sea level uncertainty budget to reflect uncertainties in the instrumental stability.

The performances of the 2-tandem phase method are very promising. However, the novel method also presents some limitations. The method is only applicable over the period encompassing the two tandem phase and does not allow the assessment of the altimeter stability outside this period. This method only allows the assessment of the stability of instrumental errors since all the other sources errors have been cancelled (e.g., geophysical and atmospherical effect, long-term errors in the POD). Therefore, no assessment of other sources of errors is made in the uncertainty budget of the mean sea level (Ablain et al., 2019; Guérou et al., 2023; Prandi et al., 2021). For these reasons, the other validation methods are complementary, although their uncertainties in the trend of sea level differences are higher.

In order to take a larger benefit of this novel cross-validation method, this involves regularly implementing double tandem phases between two successive altimetry missions in the future. The instrumental stability could be assessed over a long period. Assuming that it is theoretically possible to organise a third tandem phase between Jason-3 and S6-MF six years after the initial tandem phase, we could assess instrumental stability with uncertainties of ± 0.07 mm yr^{-1} ([16-84]% CL) on the global scale (see Fig. 5), and approximately ± 0.3 mm yr^{-1} ([16-84]% CL) at regional scales (see Fig. 4). The feasibility of conducting regular tandem phases between reference missions needs to be analysed considering the end-of-life limitations of the reference missions.

References

OSTM/Jason-2 CalVal Plan 2008, https://drive.google.com/file/d/12fkVRx4EMYug5lni-5zcidjtexanTAcc/view?usp=drive_link, 2008.

Ablain, M., Philipps, S., Picot, N., and Bronner, E.: Jason-2 Global Statistical Assessment and Cross-Calibration with Jason-1, Marine Geodesy, 33, 162–185, https://doi.org/10.1080/01490419.2010.487805, 2010.

Ablain, M., Jugier, R., Zawadzki, L., and Picot, N.: Estimating any altimeter GMSL drifts between 1993 and 2018 by comparison with tide gauges, https://www.geomatlab.tuc.gr/fileadmin/users_data/geomatlab/international_review_workshop_2018/presentations/01_Monday/Session_01/06_S1_23_Ablain_et_al.pdf, 2018.

Ablain, M., Meyssignac, B., Zawadzki, L., Jugier, R., Ribes, A., Spada, G., Benveniste, J., Cazenave, A., and Picot, N.: Uncertainty in satellite estimates of global mean sea-level changes, trend and acceleration, Earth System Science Data, 11, 1189–1202, https://doi.org/https://doi.org/10.5194/essd-11-1189-2019, publisher: Copernicus GmbH, 2019.

Ablain, M., Jugier, R., Marti, F., Dibarboure, G., Couhert, A., Meyssignac, B., and Cazenave, A.: Benefit of a second calibration phase to estimate the relative global and regional mean sea level drifts between Jason-3 and Sentinel-6a, preprint, Oceanography, https://doi.org/10.1002/essoar.10502856.1, 2020.

Barnoud, A., Pfeffer, J., Guérou, A., Frery, M., Siméon, M., Cazenave, A., Chen, J., Llovel, W., Thierry, V., Legeais, J., and Ablain, M.: Contributions of Altimetry and Argo to Non-Closure of the Global Mean Sea Level Budget Since 2016, Geophysical Research Letters, 48, e2021GL092 824, https://doi.org/10.1029/2021GL092824, 2021.

Cadier, E., Courcol, B., Prandi, P., Quet, V., Moreau, T., Maraldi, C., Bignalet-Cazalet, F., Dinardo, S., Martin-Puig, C., and Donlon, C.: Assessment of Sentinel-6MF low resolution numerical retracker over ocean: Continuity on reference orbit and improvements, Advances in Space Research, p. S0273117724011670, https://doi.org/10.1016/j.asr.2024.11.045, 2024.

Couhert, A., Cerri, L., Legeais, J.-F., Ablain, M., Zelensky, N. P., Haines, B. J., Lemoine, F. G., Bertiger, W. I., Desai, S. D., and Otten, M.: Towards the 1mm/y stability of the radial orbit error at regional scales, Advances in Space Research, 55, 2–23, https://doi.org/10.1016/j.asr.2014.06.041, publisher: Elsevier BV, 2015.

Dibarboure, G., Schaeffer, P., Escudier, P., Pujol, M.-I., Legeais, J. F., Faugère, Y., Morrow, R., Willis, J. K., Lambin, J., Berthias, J. P., and Picot, N.: Finding Desirable Orbit Options for the "Extension of Life" Phase of Jason-1, Marine Geodesy, 35, 363–399, https://doi.org/10.1080/01490419.2012.717854, 2012.

Dibarboure, G., Boy, F., Desjonqueres, J. D., Labroue, S., Lasne, Y., Picot, N., Poisson, J. C., and Thibaut, P.: Investigating Short-Wavelength Correlated Errors on Low-Resolution Mode Altimetry, Journal of Atmospheric and Oceanic Technology, 31, 1337–1362, https://doi.org/10.1175/JTECH-D-13-00081.1, 2014.

Dieng, H. B., Cazenave, A., Meyssignac, B., and Ablain, M.: New estimate of the current rate of sea level rise from a sea level budget approach, Geophysical Research Letters, 44, 3744–3751, https://doi.org/10.1002/2017gl073308, publisher: American Geophysical Union (AGU), 2017.

Dinardo, S., Maraldi, C., Daguze, J.-A., Amraoui, S., Boy, F., Moreau, T., and Picot, N.: Sentinel-6 MF Poseidon-4 Radar Altimeter In-Flight Calibration and Performances Monitoring, https://doi.org/10.24400/527896/A03-2022.3377, publisher: CNES, 2022.

Donlon, C. J., O'Carroll, A., Labroue, S., Larnicol, G., Sathyendranath, S., Merchant, C., Kwiatkowska, E., Bourg, L., Scharroo, R., and Smith, D.: Scientific Justification for a Tandem mission between Sentienl-3A and Sentinel-3B during the E1 commissioning Phase, Tech. Rep. EOP-SM/3057/CD-cd version 4.2, European Space Agency, 2016.

Donlon, C. J., Scharroo, R., Willis, J., Leuliette, E., Bonnefond, P., Picot, N., Schrama, E., and Brown, S.: Sentinel-6A/B/Jason-3 Tandem
Phase Justification and Requirements., Tech. Rep. ESA-EOPSM-S6-TN-3773 version 2.1, European Space Agency, 2020.

Donlon, C. J., Cullen, R., Giulicchi, L., Vuilleumier, P., Francis, C. R., Kuschnerus, M., Simpson, W., Bouridah, A., Caleno, M., Bertoni, R.,
Rancaño, J., Pourier, E., Hyslop, A., Mulcahy, J., Knockaert, R., Hunter, C., Webb, A., Fornari, M., Vaze, P., Brown, S., Willis, J., Desai,
S., Desjonqueres, J.-D., Scharroo, R., Martin-Puig, C., Leuliette, E., Egido, A., Smith, W. H., Bonnefond, P., Le Gac, S., Picot, N., and
Tavernier, G.: The Copernicus Sentinel-6 mission: Enhanced continuity of satellite sea level measurements from space, Remote Sensing
of Environment, 258, 112 395, https://doi.org/10.1016/j.rse.2021.112395, 2021.

Dorandeu, J., Ablain, M., Faugère, Y., Mertz, F., Soussi, B., and Vincent, P.: Jason-1 global statistical evaluation and performance assessment:
Calibration and cross-calibration results, Marine Geodesy, 27, 345–372, https://doi.org/10.1080/01490410490889094, 2004.

Ferrier, C.: Jason-3 mission overview, OSTST 2023, https://doi.org/10.24400/527896/A03-2023.3887, publisher: CNES, 2023.

Guérou, A., Meyssignac, B., Prandi, P., Ablain, M., Ribes, A., and Bignalet-Cazalet, F.: Current observed global mean sea level
rise and acceleration estimated from satellite altimetry and the associated measurement uncertainty, Ocean Science, 19, 431–451,
https://doi.org/10.5194/os-19-431-2023, publisher: Copernicus GmbH, 2023.

Hakuba, M. Z., Frederikse, T., and Landerer, F. W.: Earth's Energy Imbalance From the Ocean Perspective
(2005–2019), Geophysical Research Letters, 48, e2021GL093 624, https://doi.org/10.1029/2021GL093624, _eprint:
https://onlinelibrary.wiley.com/doi/pdf/10.1029/2021GL093624, 2021.

Henry, O., Ablain, M., Meyssignac, B., Cazenave, A., Masters, D., Nerem, S., and Garric, G.: Effect of the processing methodol-
ogy on satellite altimetry-based global mean sea level rise over the Jason-1 operating period, Journal of Geodesy, 88, 351–361,
https://doi.org/10.1007/s00190-013-0687-3, 2014.

Jugier, R., Ablain, M., Fraudeau, R., Guerou, A., and Féménias, P.: On the uncertainty associated with detecting global and local mean sea
level drifts on Sentinel-3A and Sentinel-3B altimetry missions, Ocean Science, 18, 1263–1274, https://doi.org/10.5194/os-18-1263-2022,
2022.

Marti, F., Blazquez, A., Meyssignac, B., Ablain, M., Barnoud, A., Fraudeau, R., Jugier, R., Chenal, J., Larnicol, G., Pfeffer, J., Restano, M.,
and Benveniste, J.: Monitoring the ocean heat content change and the Earth energy imbalance from space altimetry and space gravimetry,
Earth System Science Data, 14, 229–249, https://doi.org/10.5194/essd-14-229-2022, 2022.

Marti, F., Meyssignac, B., Rousseau, V., Ablain, M., Fraudeau, R., Blazquez, A., and Fourest, S.: Monitoring global ocean heat content from
space geodetic observations to estimate the Earth energy imbalance, 8th edition of the Copernicus Ocean State Report (OSR8), 4-osr8, 3,
https://doi.org/10.5194/sp-4-osr8-3-2024, publisher: Copernicus Publications, 2024.

Mertikas, S. P., Donlon, C., Matsakis, D., Mavrocordatos, C., Altamimi, Z., Kokolakis, C., and Tripolitsiotis, A.: Fiducial reference systems
for time and coordinates in satellite altimetry, Advances in Space Research, 68, 1140–1160, https://doi.org/10.1016/j.asr.2020.05.014,
2021.

Meyssignac, B., Ablain, M., Guérou, A., Prandi, P., Barnoud, A., Blazquez, A., Fourest, S., Rousseau, V., Bonnefond, P., Cazenave, A.,
Chenal, J., Dibarboure, G., Donlon, C., Benveniste, J., Sylvestre-Baron, A., and Vinogradova, N.: How accurate is accurate enough for
measuring sea-level rise and variability, Nature Climate Change, 13, 796–803, https://doi.org/10.1038/s41558-023-01735-z, 2023.

Prandi, P., Meyssignac, B., Ablain, M., Spada, G., Ribes, A., and Benveniste, J.: Local sea level trends, accelerations and uncertainties over
1993–2019, Scientific Data, 8, 1, https://doi.org/10.1038/s41597-020-00786-7, number: 1 Publisher: Nature Publishing Group, 2021.

Rudenko, S., Dettmering, D., Zeitlhöfler, J., Alkahal, R., Upadhyay, D., and Bloßfeld, M.: Radial Orbit Errors of Contemporary Altimetry
Satellite Orbits, Surveys in Geophysics, 44, 705–737, https://doi.org/10.1007/s10712-022-09758-5, 2023.

Schaeffer, P., Pujol, M.-I., Veillard, P., Faugere, Y., Dagneaux, Q., Dibarboure, G., and Picot, N.: The CNES CLS 2022 Mean Sea Surface: Short Wavelength Improvements from CryoSat-2 and SARAL/AltiKa High-Sampled Altimeter Data, Remote Sensing, 15, 2910, https://doi.org/10.3390/rs15112910, 2023.

445 Valladeau, G., Legeais, J. F., Ablain, M., Guinehut, S., and Picot, N.: Comparing Altimetry with Tide Gauges and Argo Profiling Floats for Data Quality Assessment and Mean Sea Level Studies, Marine Geodesy, 35, 42–60, https://doi.org/10.1080/01490419.2012.718226, 2012.

Watson, C. S., White, N. J., Church, J. A., King, M. A., Burgette, R. J., and Legresy, B.: Unabated global mean sea-level rise over the satellite altimeter era, Nature Climate Change, 5, 565–568, https://doi.org/10.1038/nclimate2635, number: 6 Publisher: Nature Publishing Group,
450 2015.

Watson, C. S., Legresy, B., and King, M. A.: On the uncertainty associated with validating the global mean sea level climate record, Advances in Space Research, 68, 487–495, https://doi.org/10.1016/j.asr.2019.09.053, 2021.

Zawadzki, L. and Ablain, M.: Accuracy of the mean sea level continuous record with future altimetric missions: Jason-3 vs. Sentinel-3a, Ocean Sci., 12, 9–18, https://doi.org/10.5194/os-12-9-2016, 2016.
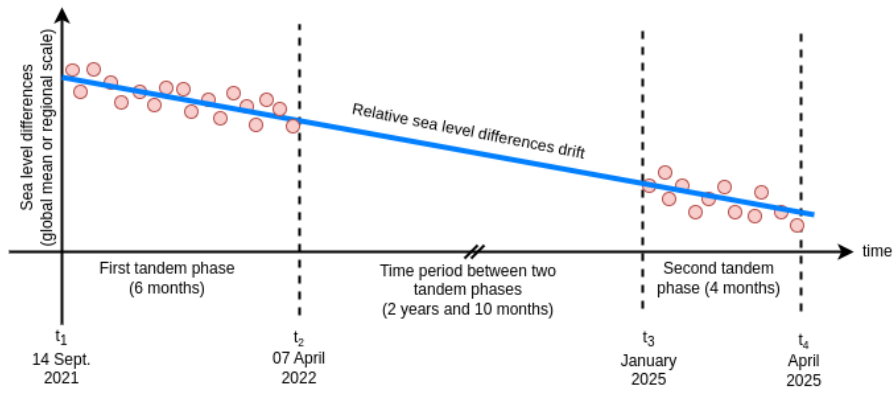
Figure 1. Basic principle of the 2-tandem phase method applied to the Jason-3 and S6-MF altimetry satellites.
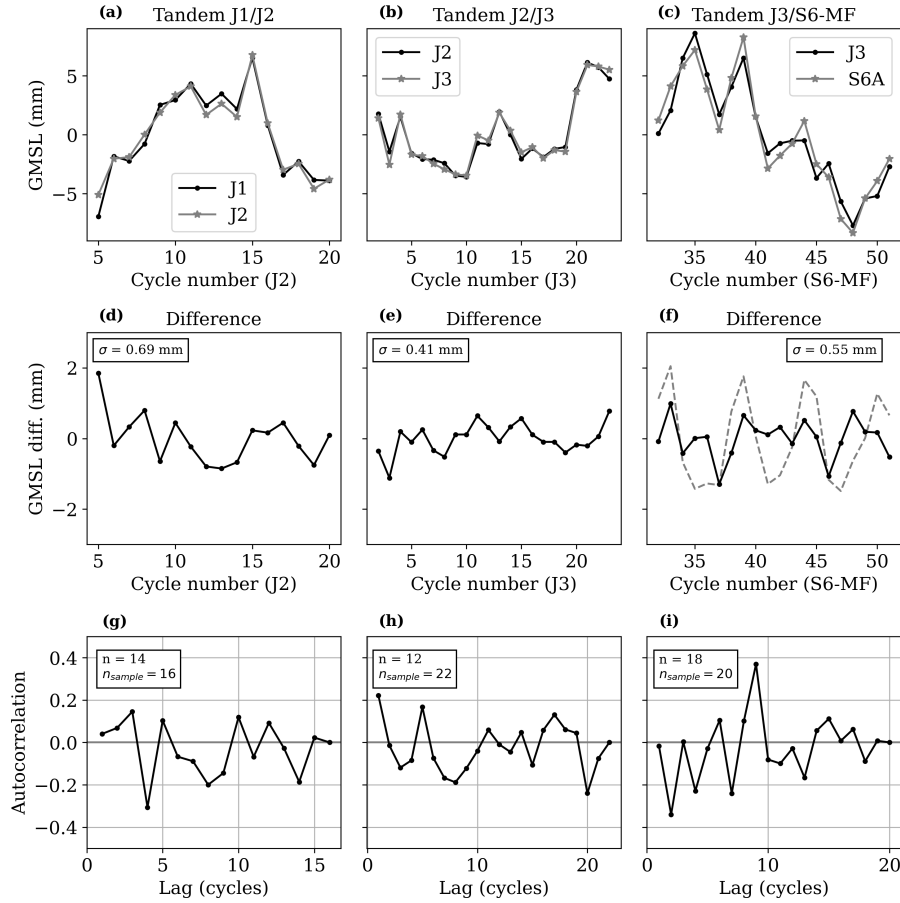
Figure 2. Panels (a-c) show GMSL records over the tandem phase between Jason-1 and Jason-2 on left (noted J1/J2), between Jason-2 and Jason-3 on the centre (noted J2/J3) , between Jason-3 and S6-MF (side B) on the right (noted J3/S6-MF); (d-f) show the GMSL record differences between the two respective missions in tandem phase. σ is the standard deviation of the GMSL differences, in (f) the dashed grey line is the GMSL differences before removal of the 60-days periodic signal; and (g-i) show the autocorrelation of the difference signal with n the number of independent measurements of the sample and n_{sample} the total number of measurements of the sample. The mean value of each time series has been removed to facilitate comparison.
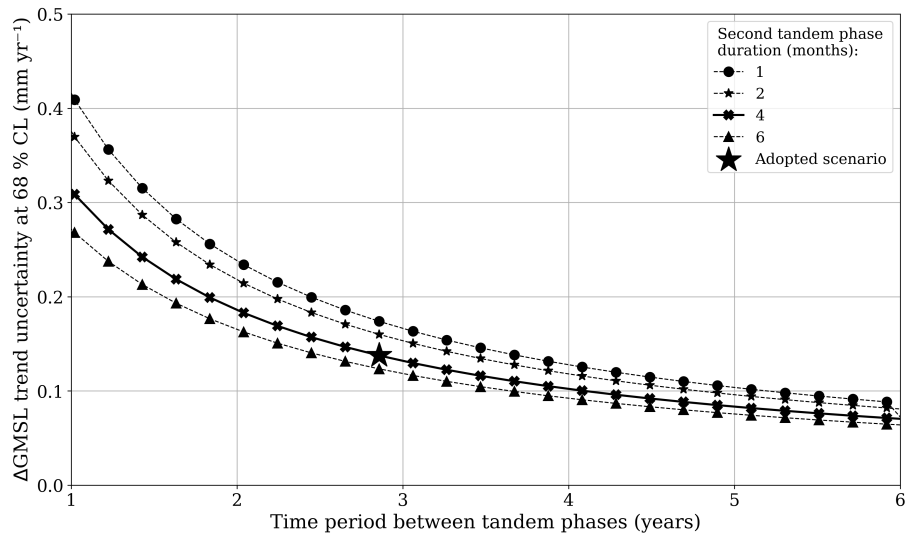
Figure 3. Evolution of the uncertainty of the trend in GMSL differences (ΔGMSL) with the time elapsed between the two tandem phases between Jason-3 and S6-MF for several durations of the second tandem phase, ranging from 1 month to 6 months. The scenario adopted by the space agencies for the second tandem phase, which is four months long and separated by two years and nine months from the first, is indicated with a star.
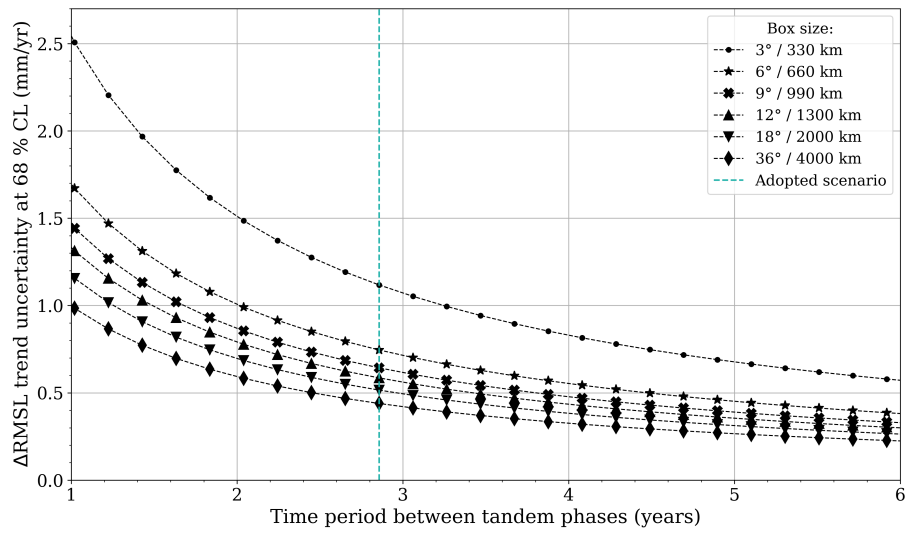
Figure 4. Evolution of the uncertainty of the trend in regional mean sea level differences (ΔRMSL) with the time period between the two tandem phases between Jason-3 and S6-MF for different cell sizes from 3°x3° (corresponding to 330 km spatial scale) to 36°x36° (corresponding to 4000 km spatial scales).
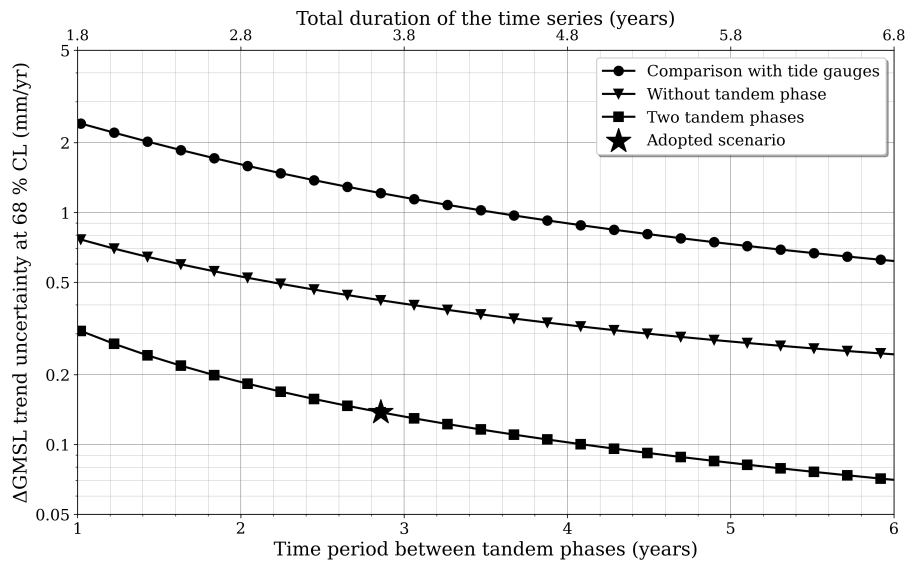
Figure 5. Evolution of the uncertainty of the trend in GMSL differences (ΔGMSL) with the time spent between the two tandem phases of Jason-3 and S6-MF for the different calibration methods: a) comparison with tide gauges ; b) inter-mission comparison without tandem; c) two tandem phases. The scenario adopted for the second tandem phase, which is four months long and separated by two years from the first one, is indicated with a star. The y-axis scale is logarithmic.
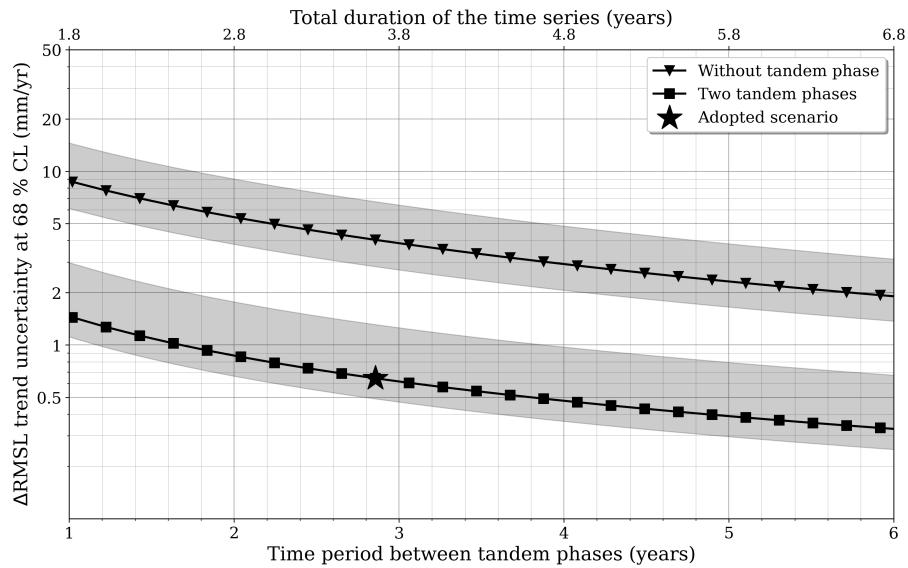
Figure 6. Evolution of the trend uncertainty of regional mean sea level differences (ΔRMSL) with the time period between the two tandem phases between Jason-3 and S6-MF for different calibration methods and cell size of 9°x9° (corresponding to 1000 km spatial scale). The envelope represents the spatial distribution of uncertainties between the 16th and 84th percentile (i.e., 1-σ) values. The y-axis scale is logarithmic. The scenario adopted for the second tandem phase, which is four months long and separated by two years and 9 months from the first one, is indicated with a star.

Table 1. Uncertainty budget of GMSL differences between two altimetry missions in tandem.

Source of errors		Time correlation of errors	Uncertainties (1-σ)
short-term time-correlated errors due to altimeter processing, precise orbit determination, etc.		short-term time-correlated errors $\lambda < 1$ month	$U_\sigma = 0.7$ mm for Jason-1/Jason-2 $U_\sigma = 0.4$ mm for Jason-2/Jason-3 $U_\sigma = 0.5$ mm for Jason-3/S6-MF[1]
		short-term time-correlated errors 1 month $< \lambda < 1$ year	$U_\sigma = 0$: no uncertainty identified
Stability of the wet tropospheric correction (WTC)		long-term time-correlated errors $\lambda < 5$ years	$U_\sigma = 0$: model WTC are used to cancel WTC errors in GMSL differences
Precise orbit determination stability	International Terrestrial Reference System (ITRF)	Linear time-correlated errors	$U_\delta = 0$: errors are cancelled between two missions in tandem
	Gravity fields	Long-term time-correlated errors $\lambda < 10$ years	$U_\sigma = 0$: errors are cancelled between two missions in tandem
GIA correction		Linear time-correlated errors	$U_\delta = 0$: errors are cancelled between two missions in tandem

[1] The uncertainty budget in this study is constructed by taking the $U\sigma$ for Jason-3/S6-MF

Table 2. Uncertainty budget of regional sea level differences between two altimetry missions in tandem. Values are provided for cell sizes ranging from 3° x 3° to 36° x 36°. They are location dependent, here we provide the median value.

Source of errors	Time correlation of errors	Uncertainty (1-σ)
Short-term time-correlated errors due to altimeter processing, precise orbit determination, oceanic variability, etc ..	Short-term time-correlated errors $\lambda < 1$ month	U_σ = 4.1 mm for box size 3°*3° U_σ = 2.7 mm for box size 6°*6° U_σ = 2.3 mm for box size 9°*9° [1] U_σ = 2.1 mm for box size 12°*12° U_σ = 1.9 mm for box size 18°*18° U_σ = 1.6 mm for box size 36°*36°
Stability of the wet tropospheric correction (WTC)	Long-term time-correlated errors $\lambda < 5$ years	U_σ = 0: model WTC are used to cancel WTC errors in sea level differences
Precise orbit determination stability	Linear time-correlated errors	$U_\delta = 0$
Instrumental stability	Linear time-correlated errors	$U_\delta = 0$
GIA correction	Linear time-correlated errors	$U_\delta = 0$

[1] The uncertainty budget in this study is constructed by taking the U_σ for box size 9°*9°.

Table A1. Uncertainty budget of the GMSL differences between two altimetry missions not in tandem (from Jugier et al., 2022).

Source of errors		Time correlation of errors	Uncertainties (1-σ)
Short-term time-correlated errors due to altimeter processing, precise orbit determination, etc.		Short-term time-correlated errors $\lambda < 2$ months	$U_\sigma \in [0.6, 0.8]^1$ mm Depending on altimetry missions
		Short-term time-correlated errors 2 months $< \lambda < 1$ year	$U_\sigma \in [0.5, 0.7]^1$ mm Depending on altimetry missions
Stability of the wet tropospheric correction (WTC)		Long-term time-correlated errors $\lambda < 5$ years	$U_\sigma = 0$: model WTC are used to cancel WTC errors in GMSL differences
Precise orbit determination stability	International Terrestrial Reference System (ITRF)	Linear time-correlated errors	$U_\delta = 0.1*\sqrt{2}$ mm yr^{-1}
	Gravity fields	Long-term time-correlated errors $\lambda < 10$ years	$U_\sigma = 0.5*\sqrt{2}$ mm yr^{-1}
GIA correction		Linear time-correlated errors	$U_\delta = 0$

[1] The uncertainty budget in this study is constructed by taking the mean value of the range : $U_\sigma = 0.7$ mm for $\lambda < 2$ months and $U_\sigma = 0.6$ mm for 2 months $< \lambda < 1$ year.

Table B1. Uncertainty budget of the MSL differences between two altimetry missions not in tandem (from Jugier et al., 2022). Values are provided for 9° × 9° box sizes within a 16th-percentile and 84th-percentile interval.

Source of errors	Time correlation of errors	Uncertainties (1-σ)
Short-term time-correlated errors due to altimeter processing, precise orbit determination, etc.	Short-term time-correlated errors $\lambda < 2$ months	$U_\sigma \in [0.6, 0.8]^{1}$ mm Depending on altimetry missions
	short-term time-correlated errors 2 months $< \lambda < 1$ year	$U_\sigma \in [0.5, 0.7]^{1}$ mm Depending on altimetry missions
Stability of the wet tropospheric correction (WTC)	Long-term time-correlated errors $\lambda < 5$ years	$U_\sigma = 0$: model WTC are used to cancel WTC errors in GMSL differences
Precise orbit determination stability	Linear time-correlated errors	$U_\delta = 0.33*\sqrt{2}$ mm yr^{-1}
Gravity fields	Long-term time-correlated errors $\lambda < 10$ years	$U_\sigma = 0.5*\sqrt{2}$ mm yr^{-1}
GIA correction	Linear time-correlated errors	$U_\delta = 0$

[1] The uncertainty budget in this study is constructed by taking the median value : $U_\sigma = 9.4$ mm for $\lambda < 2$ months and $U_\sigma = 4.9$ mm for 2 months $< \lambda < 1$ year.

Table C1. Uncertainty budget of GMSL differences between altimeter measurements and tide gauges data from GLOSS/CLIVAR network (from Ablain et al. (2018)).

Source of errors	Time correlation of errors	Uncertainty (1-σ)
Short-term time-correlated errors due to tide gauge and altimeter measurement errors, but also due to the collocation of both datasets.	Short-term time-correlated errors $\lambda < 6$ months	U_σ = 4.0 mm for T/P U_σ = 3.5 mm for Jason-1 U_σ = 2.3 mm for Jason-2/Jason-3[1]
	Short-term time-correlated errors 6 months $< \lambda <$ 1 year	U_σ = 1.0 mm for T/P U_σ = 0.7 mm for Jason-1 U_σ = 0.5 mm for Jason-2/Jason-3[1]
Long-term time correlated errors due to tide gauge networks (e.g. averaging method to take into spatial distribution), long-term stability of tide gauge time serie	Long-term time-correlated errors $\lambda < 3$ years	$U_\delta = 0.1*\sqrt{2}$ mm yr^{-1}
	Long-term time-correlated errors $\lambda < 10$ years	U_σ = 1.0 mm
Linear time-correlated over all the altimetry period due to the VLM errors of the tide-gauge network.	Linear time-correlated errors	U_δ = 0.2 mm yr^{-1}

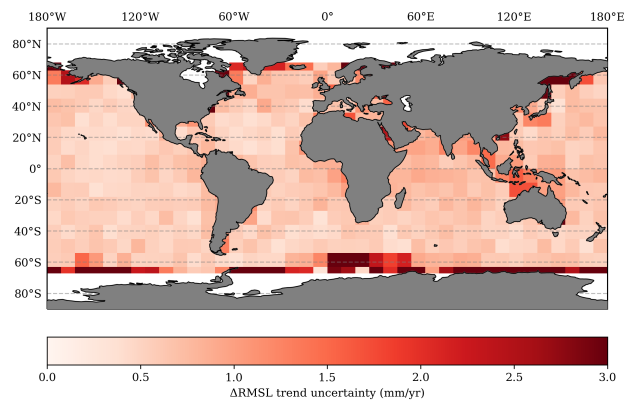[1] The uncertainty budget in this study is constructed by taking the U_σ for Jason-2/Jason-3

Figure A1. Uncertainties of the trend in regional mean sea level differences of the 2-tandem phase method for a 9° x 9° cell size and for a 2-year and 9 month time spent between the two Jason-3 and S6-MF tandem phases.